Journal of Biomolecular NMR, 7 (1996) 190–206
ESCOM

J-Bio NMR 342

Determination of sugar conformations by NMR in larger DNA duplexes using both dipolar and scalar data: Application to d(CATGTGACGTCACATG)$_2$

Maria R. Conte[a], Christopher J. Bauer[b,*] and Andrew N. Lane[a,**]

[a]*Division of Molecular Structure and* [b]*Biomedical NMR Facility, National Institute for Medical Research, The Ridgeway, Mill Hill, London NW7 1AA, U.K.*

Received 28 November 1995
Accepted 26 February 1996

Keywords: Sugar conformation; Scalar coupling; NOEs; ATF-2

Summary

Different methods for determining sugar conformations in large oligonucleotides have been evaluated using both J-coupling and NOE data. In order to simulate COSY spectra, reliable estimates of line widths are required. We have measured $T_{1\rho}$ ($=T_2$) values for a large number of protons of the hexadecamer d(CATGTGACGTCACATG)$_2$ using a new two-dimensional NMR experiment (T1RHOSY) to provide baseline information for the simulations. Both DQF-COSY and P.E.COSY cross-peaks have been systematically simulated as a function of line width, digitisation and signal-to-noise ratio. We find that for longer correlation times ($\tau \geq 5$ ns), where line widths are comparable to or larger than active couplings, only $\sum_{1'}$ ($^3J_{1'2'}+{}^3J_{1'2''}$) is reasonably accurately determined (within ± 1 Hz). Under these conditions, additional information is needed to determine the sugar conformation. We have used apparent distances H1'-H4' and H2''-H4', which provide a range of P_S over an interval of ca. 20°. Complete analysis of time courses for intraresidue NOEs, with and without coupling constants, has also been evaluated for determining nucleotide conformations. Whereas P_S is poorly determined in the absence of both intrasugar NOEs and coupling constants, the range of solutions is decreased when intrasugar NOEs and $\sum_{1'}$ are also available. DQF-COSY, P.E.COSY and NOESY spectra at different mixing times of the hexadecamer d(CATGTGACGTCACATG)$_2$ were recorded at three temperatures. A detailed analysis of the NOEs and coupling constants provided estimates of the sugar conformations in the hexadecamer. At 50 °C, the sugar conformations are well determined by the scalar and dipolar data, with pseudorotation phase angles of 126–162° and mole fractions of the S conformation (f_S) of 0.86 ± 0.05. There was no statistically significant difference between f_S for the purines and the pyrimidines, although there was a small tendency for P_S of the purines to be larger than those of the pyrimidines. At 25 °C, the sugar conformations were much less well determined, although the estimates of f_S were the same within experimental error as at 50 °C. The experimental and theoretical results provide guidelines for the limits of conformational analysis of nucleic acids based on homonuclear NMR methods.

Introduction

The conformation of the nucleotide units in DNA determines the overall position of the backbone. For a rigid nucleotide unit, the conformation can be described with only three parameters, namely the glycosidic torsion angle, χ, which determines the relative position of the base with respect to the sugar, and the pseudorotation phase angle, P, and the maximum amplitude ϕ_m, which determine the exact conformation of the sugar moiety. In principle, these parameters can be determined using a combination of scalar couplings (Van Wijk et al., 1992) and NOEs between base and sugar protons. The number of independent data then greatly exceeds the number of parameters (three), so that the problem is overdetermined. However, if the sugars exist as a mixture of two or more

*Present address: Credit Suisse Financial Products, 1 Cabot Square, London E14 4QJ, U.K.
**To whom correspondence should be addressed.

pucker states (Rinkel and Altona, 1987; Van de Ven and Hilbers, 1988; Schmitz et al., 1990; Van Wijk et al., 1992; Wijmenga et al., 1993), and the glycosidic torsion angle is not necessarily the same in each pucker state, then there are many more parameters to be determined. For a two-state sugar equilibrium, there are seven parameters to be determined, namely the pseudorotation phase angles and maximum amplitudes of the two sugar conformations, the mole fraction of each state, f_S, and the two values of the glycosidic torsion angle, $\chi(S)$ and $\chi(N)$. In practice it is usually assumed that $\phi_m(N) = \phi_m(S)$ and $P_N = 9°$.

In principle, vicinal coupling constants required to determine accurate sugar puckers should be available from a variety of 2D NMR techniques that present J-coupling information in a different fashion. The sugar conformations can be more reliably analysed using sums of coupling constants which contain the same information as individual three-bond couplings (Rinkel and Altona, 1987; Van Wijk et al., 1992), because of difficulties in deriving individual coupling constants in the presence of relatively broad resonances, and the possible complication of cross-correlation effects between scalar and dipolar coupling for larger molecules (Zhu et al., 1994; Norwood, 1995). The sums of coupling constants, obtained from the separation of the outermost components of a multiplet, are also immune to the effects of strong coupling.

In short oligonucleotides (less than ca. 12 residues), the line widths of even the broadest resonances (H2' and H2") are sufficiently small compared with the coupling constants, so that most of the scalar couplings can be obtained directly from 1D and DQF-COSY spectra. In larger duplexes or triplexes, however, the line widths can become larger than the scalar couplings, which requires a more sophisticated spectral analysis to obtain the desired couplings (Gochin et al., 1990; Schmitz et al., 1990, 1992).

In addition, spectral overlap often prevents a complete set of couplings from being obtained. The scalar couplings then have to be supplemented by additional information, such as the NOEs between sugar protons and between base and sugar protons (Conte et al., 1995). Furthermore, in order to analyse the couplings of resolved cross-peaks in DQF-COSY or P.E.COSY spectra, it is necessary to simulate the expected fine structure for the experimental conditions. In addition to the coupling constants, an accurate value of the line width must be supplied (Gochin et al., 1990; Schmitz et al., 1990,1992). There are alternative methods for obtaining scalar coupling information, such as heteronuclear experiments (Eberstadt et al., 1995) and measurements of peak intensities in TOCSY spectra (Van Duynhoven et al., 1992). As heteronuclear labelling techniques in DNA are still difficult, these methods were not available to us. The TOCSY method is also very compute-intensive, and the effects of relaxation have to be evaluated as well. For these reasons, DQF-COSY and P.E.COSY remain the most commonly used experiments at present.

As part of a study on the interaction of the leucine zipper protein ATF-2, an activating transcription factor in mammalian development (Tassios and LaThangue, 1990) with its cognate DNA target site, we have assigned the ^{1}H NMR spectrum of d(CATGTGACGTCACATG)$_2$ (M.R. Conte and A.N. Lane, unpublished results), which contains the core ATF recognition site (underlined) and flanking sequences for ATF-2 (Jones and Lee, 1991). To obtain detailed information about the sugar conformations in this 16-base-pair oligodeoxynucleotide, we have recorded DQF-COSY and P.E. COSY spectra at different temperatures to assess the influence of line width on the spectra. We have simulated peak shapes using the program Gamma (Smith et al., 1994), which includes relaxation effects, and the estimated spin–spin couplings have been compared with those obtained from measurements of splittings in cross sections of 2D spectra. To investigate the variation of line widths for different proton types and sequence dependence, we have developed a two-dimensional rotating-frame method, which provides estimates of the intrinsic relaxation rate constants for coupled protons.

We have systematically examined the influence of line widths, noise and digital resolution on the estimation of coupling constants from DQF-COSY and P.E.COSY. The simulations provide guidelines for determining coupling constants and limitations on the methods. The use of NOE distance data for determining sugar conformations (Van de Ven and Hilbers, 1988; Wijmenga et al., 1993) and NOE time courses (Lane, 1990) has been previously discussed in detail. Here we have evaluated the use of simultaneously fitting scalar coupling data and NOEs or distances for analysing nucleotide conformations in order to discover how much data are required to determine the sugar conformation and glycosidic torsion angle in the presence of conformational averaging.

Materials and Methods

Materials

The 16-mer d(CATGTGACGTCACATG) was synthesised and purified using reverse-phase HPLC by Oswell (Edinburgh, U.K.).

The sample was dissolved in an aqueous buffer (5 mM sodium phosphate, 100 mM KCl, 0.1 mM EDTA, pH = 7) and annealed by slow cooling from 80 °C. After lyophilisation, the sample was redissolved in 0.6 ml D_2O. The final concentration of the DNA was 1.6 mM in duplex.

For NMR experiments 2,2-dimethyl-2-silapentane-5-sulphonate (DSS) was used as an internal chemical shift reference. NMR experiments were carried out at 11.75 T

and 14.1 T, using Varian UnityPlus and Unity spectrometers, respectively.

Methods

Phase-sensitive DQF-COSY, NOESY and TOCSY spectra were recorded at 25 °C, 40 °C and 50 °C with acquisition times in t_1 and t_2 of 0.07 and 0.7 s, respectively. The data were padded with zeros to 16 384 × 2048 complex points, and multiplied by a shifted Gaussian function in both dimensions prior to Fourier transformation. Phase-sensitive spectra were recorded using the method of States et al. (1982). Isotropic mixing in the TOCSY experiments was obtained using MLEV-17 (Bax and Davis, 1985), typically providing a spin-lock field strength of 8 kHz for a duration of 50 ms. The modification suggested by Griesinger et al. (1988) for attenuating ROESY cross-peaks was applied.

The P.E.COSY experiment was recorded as described by Bax and Lerner (1988), using a flip angle of 36°. The J-scaled double-quantum-filtered spectrum was acquired as described previously (Bax and Lerner, 1988).

Estimates of spin–spin relaxation rates for protons of which the resonances are resolved in one-dimensional NMR spectra were obtained by measuring T_1 in the rotating frame (Freeman and Hill, 1971) at 25 °C, 40 °C and 50 °C, using the transmitter for both low- and high-power pulses. The duration of the spin-lock period, τ, was increased from 1 to 300 ms at 25 °C, from 1 to 500 ms at 40 °C and from 1 to 600 ms at 50 °C, in 15 unequally spaced steps. The data were analysed by nonlinear regression to:

$$M(\tau) = M^0 \exp(-R_{1\rho}\,\tau) \qquad (1)$$

where $M(\tau)$ is the magnetisation at time τ, M^0 is the magnetisation at time $\tau = 0$, and $R_{1\rho}$ is the spin-lattice relaxation rate constant in the rotating frame. The identity $R_2 = R_{1\rho}$ is assumed (Allerhand et al., 1965; Farmer et al., 1988; Lane et al., 1993). To determine the $R_{1\rho}$ values of a larger number of protons, we have used a two-dimensional version of the experiment. In the 2D rotating-frame T_1 experiment, which we call T1RHOSY, the following pulse sequence was used:

$$D1\text{-}90x\text{-}SLy(\tau)\text{-}t_1\text{-}[90\text{-}t_m\text{-}90]\ t_2 \qquad (2)$$

During the acquisition time t_2 and the delay D1, magnetisation relaxes along the z-axis. The 90x-SLy(τ) segment converts z magnetisation into y magnetisation, which is then allowed to relax in the rotating frame for a period τ. The y magnetisation that remains at the end of the spin-lock period depends on the relevant $T_{1\rho}$ values of the different spins. Free precession during t_1 generates the indirect frequency domain, and magnetisation is then mixed by the subsequence shown in square brackets. There are several possibilities for the mixing sequence, such as another spin-lock period (TOCSY-style experiment), a pair of 90° pulses differing in phase by 90° (COSY-type mixing) or the one shown in Eq. 2, which provides NOESY mixing. We have chosen to use the NOESY mixing sequence, as it allows detection of correlations between protons that may or may not be scalar coupled. If an optimal mixing time t_m is chosen, good sensitivity can be obtained, and there are multiple cross-peaks to be chosen for each proton type.

Eight NOESY experiments (T1RHOSY) were performed with spin-lock times of 1, 10, 20, 30, 50, 80, 120 and 150 ms with a fixed spin-lock field strength of 8 kHz. The spectra were recorded sequentially at 40 °C at 11.75 T. In all the experiments the NOESY mixing time was 300 ms, and acquisition times were 0.05 s and 0.4 s in t_1 and t_2, respectively. Data matrices were multiplied by a nonshifted Gaussian function in both dimensions and zero-filled to 8192 by 1024 points. The data were analysed by fitting cross-peak intensities as a function of spin-lock duration to Eq. 1.

H1'-H4' and H2"-H4' distances (see below) were determined for each sugar, from the ratio of H1'-H4' and H1'-H2" peak areas, and of H2"-H4' and H2"-H1' peak areas, respectively, from NOESY spectra acquired with short mixing times (30, 50, 100 ms) at different temperatures. The ratio of the peak area of each pair of cross-peaks is proportional to the ratio of the NOE intensities (since each pair of peak areas is taken from the same cross section), so that distances could be calculated by using the fixed distance for H1'-H2" of 0.235 ± 0.005 nm. Best estimates were then obtained by extrapolating the empirical distances to zero mixing time.

Simulations

DQF-COSY and P.E.COSY cross-peaks were simulated using the program Gamma (Smith et al., 1994) for a complete deoxyribose spin system. This program produces a file of free induction decays, given frequencies, coupling constants and T_2 values. The digital resolution and couplings appropriate to different sugar conformations (or mixtures of conformations) were varied, as were the line widths of the different protons. The line widths were taken from experimental values (see above) over the observed range, and including the ca. 1-Hz magnetic field inhomogeneity present in the experiments. The effects of strong coupling were investigated for the smallest shift differences between coupled spins that were observed experimentally. As the results of the calculations were not significantly different compared to the weak coupling approximation, we used weak coupling for most of the systematic calculations. Spectra were calculated for 20 conformations: $f_S = 1.0$, 0.9, 0.8 and 0.7 at each value of $P_S = 180$, 162, 144, 117 and 99° for each set of line widths. In all cases, $^2J_{2',2''}$ was set to −14.2 Hz.

TABLE 1
$R_{1\rho}$ VALUES MEASURED AT DIFFERENT TEMPERATURES FOR RESOLVED PROTONS OF d(CATGTGACGTCACATG)$_2$

Proton	$R_{1\rho}$ (s^{-1})		
	298 K	313 K	323 K
C1 H6	nd[a]	7.1	nd
A2 H8	15.6	10.0	7.3
G4 H8	nd	9.3	7.0
T5 H6	23.9	15.0	12.3
G6 H8	nd	8.6	6.9
A7 H8	15.0	10.3	8.3
C8 H5	6.8	4.9	3.7
G9 H8	15.2	9.3	nd
C11 H6	7.5	16.9	13.2
C11 H5	7.0	5.7	4.1
A12 H8	nd	9.9	8.0
C13 H5	6.7	5.7	3.6
T15 H6	21.9	14.0	10.4
G16 H8	9.4	5.3	4.6
A2 H1'	15.6	12.8	9.5
T15 H1'	12.4	7.8	5.5
C8 H1'	nd	8.0	5.5
A2 H2"	65.3	31.8	20.3
G4 H3'	15.1	10.3	8.6
G9 H3'	14.8	10.4	9.2
C1 H3'	8.6	3.8	3.4
A12 H4'	16.1	12.0	11.0

$R_{1\rho}$ values were determined from 1D rotating-frame experiments, as described in the text.
[a] nd = not determined.

Weakly coupled spectra were also simulated using an in-house program that generates cross sections through cross-peaks for NOESY and COSY spectra, given chemical shifts, and line widths for the protons of nucleotides of a given conformation, i.e., values of P_S and P_N, the pseudorotation phase angle for the S and N conformers, respectively, ϕ_m, the amplitude of the pseudorotation, and f_S, the mole fraction of the S conformer. The appropriate coupling constants are generated via the Karplus equation (cf. Van Wijk et al., 1992). The effect of noise and digitisation along F2 was examined, using a random number generator to produce white noise of the desired amplitude. More detailed analysis of the influence of noise was made by synthesising two-dimensional data sets of Gaussian noise (Press et al., 1986) consisting of the same number of points as in the two-dimensional data sets produced by Gamma. The data and noise files were added using a multiplier to produce different signal-to-noise ratios.

A program (PFIT) was written to analyse sugar conformations using experimentally derived coupling constants and proton–proton distances. The program generates all coupling constants for deoxyriboses using Altona's formalism and the parameterisation given by Wijmenga et al. (1993) as a function of P_S, P_N, ϕ_m and f_S. For a given set of parameters, the program also provides the distances H1'-H4' and H2"-H4', which are sensitive to sugar geometry (Van de Ven and Hilbers, 1988). In the presence of conformational averaging between N and S states, these 'distances' are calculated as follows:

$$r_{ij}^{-6} = S^2[f_S / r(S)_{ij}^6 + (1 - f_S) / r(N)_{ij}^6] \quad (3)$$

where r(S) and r(N) are the actual distances in the S and N states, respectively, f_S is the mole fraction of the S state and S^2 is an order parameter. In this formalism it is assumed that motions other than overall tumbling are very rapid, such that the spectral density functions are simply scaled by the order parameter (cf. Lipari and Szabo, 1982; Lane and Forster, 1989). Using the methods described by Tropp (1980), order parameters for specified motions of any vector can be calculated in a straightforward manner (Lane and Forster, 1989). Furthermore, experimental values of order parameters for sugar proton–proton vectors have been measured in DNA fragments (Lane and Forster, 1989; Lane, 1991), calculated from molecular dynamics trajectories (Koning et al., 1991), and from C-H relaxation (Lane, 1991; Borer et al., 1994). Sugar repuckering is one of many possible motions,

TABLE 2
$R_{1\rho}$ VALUES FOR d(CATGTGACGTCACATG)$_2$ AT 40 °C DETERMINED WITH T1RHOSY

Nucleotide	$R_{1\rho}$ (s^{-1})					
	H8/H6	H1'	H2'	H2"	H3'	H4'
C1	8.5	5.5	15.4	12.1	nd[a]	nd
A2	10.1	13.3	29.3	30.2	12.9	10.1
T3	17.2	10.9	10.2	29.0	31.7	11.9
G4	nd	11.3	30.8	31.9	10.3	12.8
T5	15.3	8.2	30.5	27.0	11.7	nd
G6	nd	9.1	32.4	34.8	11.1	10.5
A7	11.1	14.0	31.0	33.3	11.9	nd
C8	19.8	8.2	27.1	24.9	10.0	nd
G9	nd	9.5	29.9	36.5	10.9	12.1
T10	19.5	10.3	nd	33.5	13.0	nd
C11	17.1	7.5	30.0	24.9	nd	nd
A12	10.2	14.0	31.8	33.1	11.9	11.0
C13	17.8	8.5	27.3	25.9	12.3	nd
A14	10.3	11.6	27.6	32.6	10.2	11.9
T15	14.8	8.2	27.4	23.3	10.2	nd
G16	5.3	7.1	13.2	17.1	4.2	nd
mean	13.6	10.3	29.7	30.3	11.4	11.4
sd	4.4	1.7	4.1	1	0.3	0.9
Y	14.4	8.7	28.3	27.3	11.3	–
	1.8	1	1.3	3.5	1	–
R	10.4	11.8	30.4	33.2	11.3	–
	0.4	1.9	1.5	1.9	0.9	–

Values were determined as described in the text. Because of the small number of values for H4', the breakdown into purines and pyrimidines has not been given. Mean values do not include the terminal nucleotides.
[a] nd = not determined.

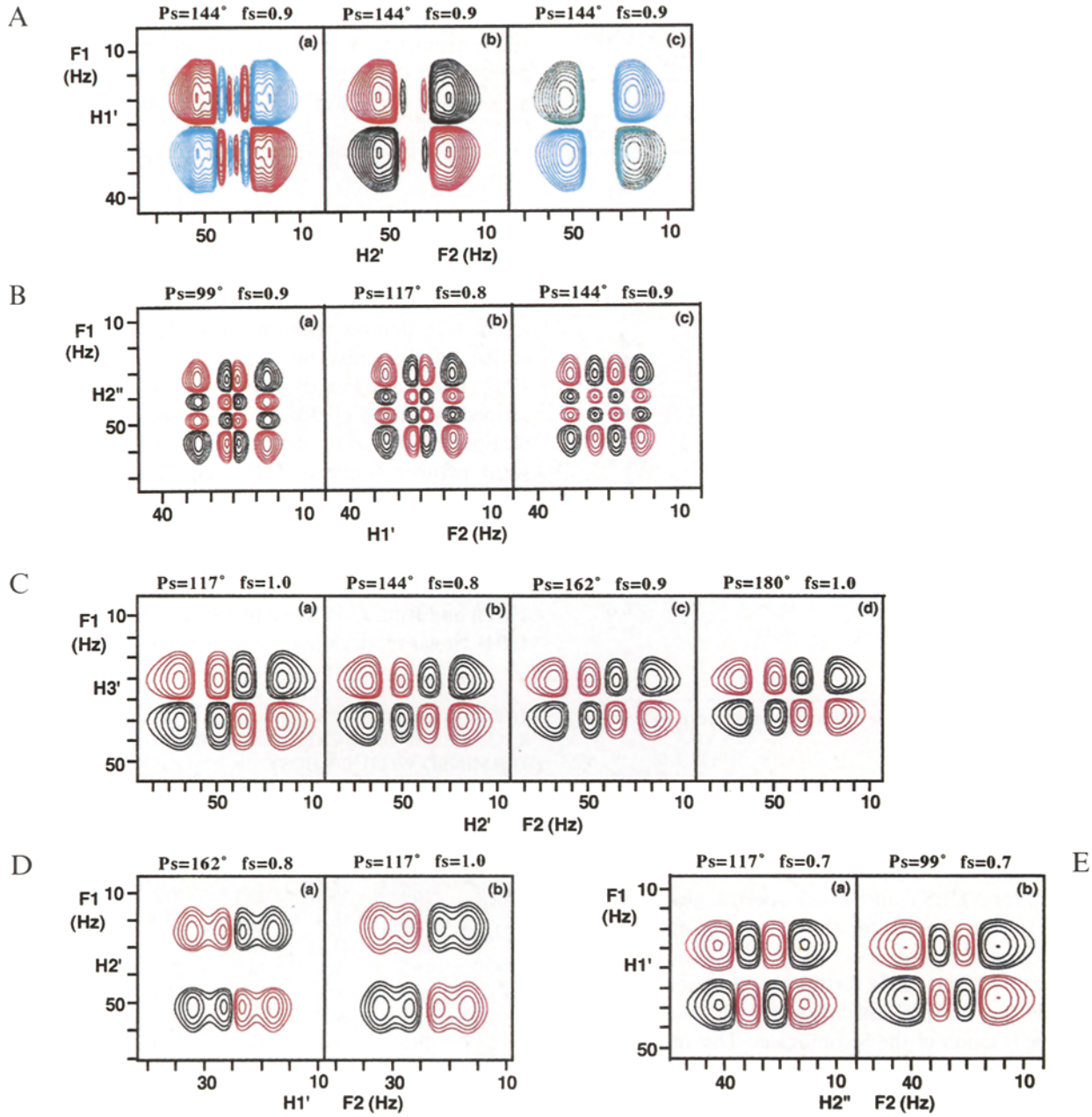

Fig. 1. Simulated DQF-COSY spectra, demonstrating the effect of line width. H1'-H2' cross-peaks were simulated using the program Gamma, as described in the Methods. (A) H1'-H2' cross-peaks for $P_S = 144°$, $f_S = 0.9$. (a) line-width set (I); (b) line-width set (II); (c) line-width set (IV). (B) H2"-H1' cross-peaks for: (a) $P_S = 99°$, $f_S = 0.9$ (I); (b) $P_S = 117°$, $f_S = 0.8$ (II); (c) $P_S = 144°$, $f_S = 0.9$ (III). (C) H3'-H2' cross-peaks for: (a) $P_S = 117°$, $f_S = 1.0$ (II); (b) $P_S = 144°$, $f_S = 0.8$ (III); (c) $P_S = 162°$, $f_S = 0.9$ (IV); (d) $P_S = 180°$, $f_S = 1.0$ (IV). (D) H2'-H1' cross-peaks for: (a) $P_S = 162°$, $f_S = 0.8$ (III); (b) $P_S = 117°$, $f_S = 1.0$ (IV). (E) H1'-H2" cross-peaks for: (a) $P_S = 117°$, $f_S = 0.7$ (I); (b) $P_S = 99°$, $f_S = 0.7$ (III). Sets of line widths (in Hz): (I) H1' = 3.5, H2' = 7.5, H2" = 7.5, H3' = 3.8, H4' = 4.4; (II) H1' = 3.6, H2' = 9.6, H2" = 8.4, H3' = 4.2, H4' = 4.2; (III) H1' = 4.2, H2' = 10.2, H2" = 9.9, H3' = 4.5, H4' = 4.5; (IV) H1' = 5.5, H2' = 11.2, H2" = 11.7, H3' = 4.8, H4' = 4.8.

the effect of which depends on the mole fraction f_S. Generalised order parameters for this specific motion are high for H1'-H4' and H2"-H4' (Koning et al., 1991). However, sugar repuckering has been shown not to be the sole determinant of the observed order parameters (Lane and Forster, 1989). Measured and calculated values of S^2 for various sugar proton vectors of nonterminal residues are typically in the range 0.7–0.9 (Lane and Forster, 1989; Koning et al., 1991; Lane, 1991), and as Eq. 3 shows will have a fairly small effect on the apparent distance. Order parameters for the H1'-H2" vectors in the present hexadecamer measured as previously described (Lane and Forster, 1989) are 0.7 ± 0.1. Order parameters for the desired H1'-H4' and H2"-H4' vectors cannot be determined from the data used to derive distances. However, calculations using Tropp's model show that motions such as a

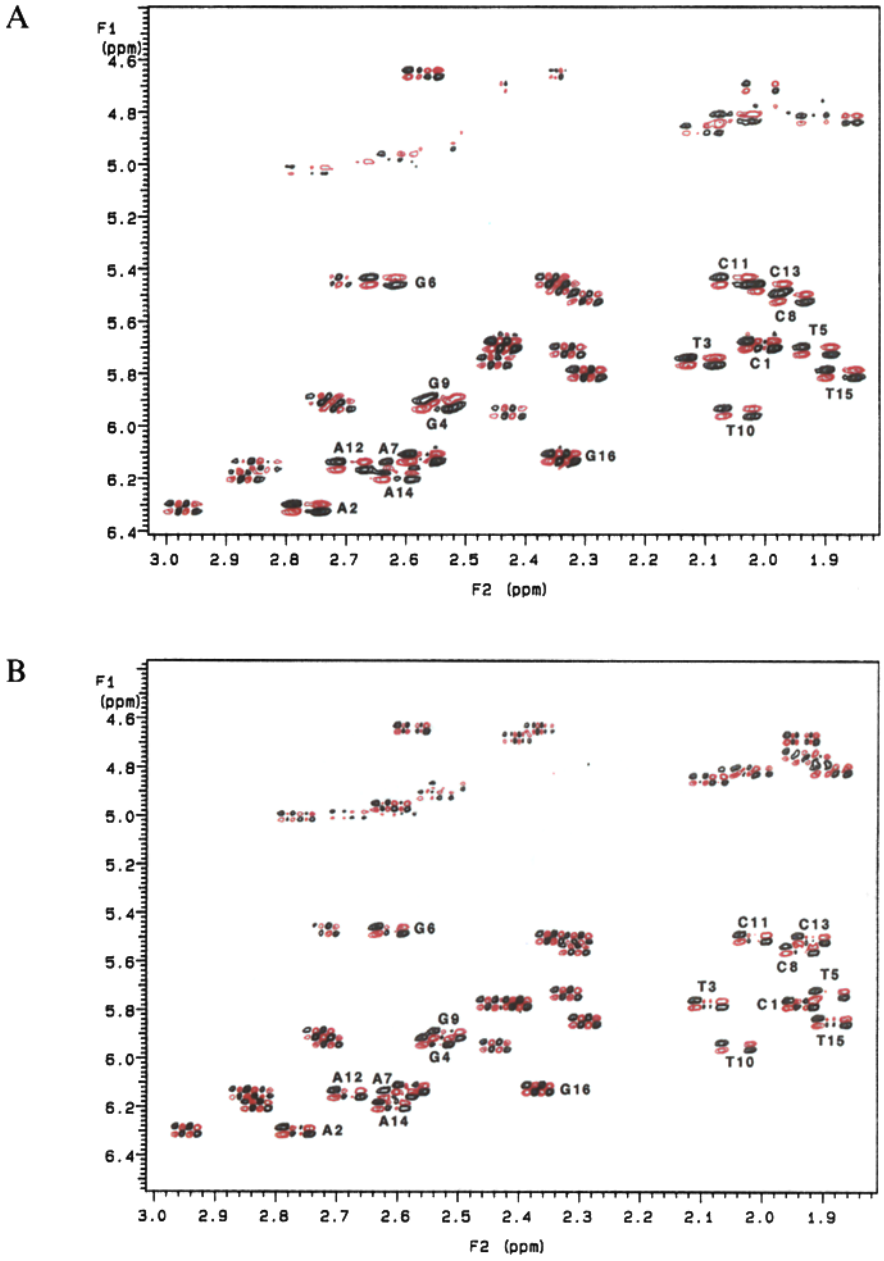

Fig. 2. DQF-COSY spectra of d(CATGTGACGTCACATG)$_2$ at two different temperatures. The spectra were at 14.1 T recorded at 25 °C and 50 °C, as described in the Methods. The data matrices consisted of 16 384 complex points in t_2 and 2048 complex points in t_1, to give final digital resolutions of 0.67 and 5.37 Hz/point in F2 and F1, respectively. The free induction decays were multiplied by shifted Gaussian functions in both dimensions. (A) Spectrum at 25 °C; and (B) spectrum at 50 °C.

fluctuation of the sugar position of ± 20° by rotation about the glycosidic bond affect H1'-H2", H1'-H4' and H2"-H4' in a similar way. Despite the uncertainty in S^2, inclusion of the order parameter serves as a reminder that this additional uncertainty in distances precludes the use of very tight distance constraints.

For each parameter set, the mean fractional error E_m is calculated according to:

$$E_m = (1/N_J)\sum|J(obs) - J(calc)| / J(obs) + (1/N_r)\sum|r(obs) - r(calc)| / r(obs) \quad (4)$$

where N_J and N_r are the numbers of J values and distances, respectively. The results are tabulated. All solutions that pass a cutoff criterion for fitting are accepted as valid solutions. Either individual coupling constants or sums of coupling constants can be used as input. Simulations were performed using sets of coupling constants chosen with random variation of up to 1 Hz from the true values, with and without distance constraints. Typical limits on the distances were –20/+50 pm for H1'-H4' and –20/+80 pm for H2"-H4'.

Because distances derived from NOEs may be affected

by spin diffusion, we have also used the program NUCFIT (Lane, 1990) to determine nucleotide conformations. This program includes effects of spin diffusion, conformational averaging in the nucleotides, motional anisotropy and any effects on intensities due to incomplete longitudinal relaxation (Lane and Fulcher, 1995). It also accepts coupling constants and NOE time courses for any desired protons. In addition to the coupling constants and the H4'-H1',H2" NOEs, the base H8/H6-H1',H2',H2",H3' NOEs provide information about the glycosidic torsion angle and to some extent the value of f_S (in particular the H8/H6-H3' NOE). We have used the combined search and least-squares fitting routine in NUCFIT to evaluate the precision of the derived values of P_S, f_S and χ, using different portions of the data, i.e., with and without coupling constants and with or without the H4'-H1',H2" NOEs.

Results

Simulation of DQF-COSY and P.E.COSY spectra

The appearance of cross-peaks in COSY experiments depends on several factors in addition to the magnitude and number of scalar couplings, such as the line width, digital resolution and signal-to-noise ratio. To assess the influence of line width on the splittings as a function of conformation (i.e., coupling constants), it can be helpful to simulate the spectra under conditions approximating those of the experiment. This approach has been used extensively by James' group (Gochin et al., 1990; Schmitz et al., 1990,1992) and others (Majumdar and Hosur, 1992; Schultze et al., 1994). However, to approximate the experimental conditions, it is necessary to supply appropriate values of the line widths of all resonances involved in the calculation. We have therefore made measurements of the line width of resolved resonances, and in addition we have developed a two-dimensional method for experimentally measuring T_2 for the hexadecamer d(CATGTGACGTCACATG)$_2$

Determination of spin–spin relaxation rates in d(CATGTGACGTCACATG)$_2$

We have measured the correlation time of the cytosine H6-H5 vectors at 25 °C and 40 °C from NOE build-up curves (Lane et al., 1986). We obtained values of 6.1 ns at 25 °C and 3.6 ns at 40 °C. Using these values for the correlation time, we have calculated the expected dipolar relaxation rate constants for B-DNA with the program NUCFIT (Lane, 1990; Lane and Fulcher, 1995). Typical values of R_2 calculated for nonterminal residues are in the range 14–15 s^{-1} for A/G H8, 19 s^{-1} for T H6, ≈ 7 s^{-1} for H1', 26–29 s^{-1} for H2', 31–34 s^{-1} for H2", ca. 11 s^{-1} for H3' and ca. 7 s^{-1} for H4' at 500 MHz for a rotational correlation time of 3.6 ns. These values are comparable to experimental estimates for most protons, although H1' and H4' are significantly smaller than the measured values (cf. Tables 1 and 2).

We have measured R_1 in the rotating frame to provide an estimate of the spin–spin relaxation, based on the approximation valid for macromolecules that $R_{1\rho} = R_2$ when using a strong spin-lock field strength (Allerhand et al., 1965; Farmer et al., 1988). This experiment is less susceptible to artefacts from scalar coupling than the

TABLE 3
ERRORS IN COUPLING CONSTANTS DERIVED FROM SPLITTINGS IN SIMULATED DQF-COSY SPECTRA: EFFECT OF LINE WIDTH

P_S (°)	f_S	LW[a]	$\Delta\Sigma_{1'}$		$\Delta J_{1'2'}$		$\Delta J_{1'2''}$		$\Delta\Sigma_{2'}$		$\Delta\Sigma_{2''}$
			2'1'	2"1'	2'1'	2"1'	2'1'	2"1'	1'2'	3'2'	1'2"
162	1.0	I	0.03	0.07	0.05	0.0	−0.07	0.08	−0.55	0.79	−0.03
		II	−0.04	0.14	0.01	0.03	−0.05	0.1	−1.42	1.20	0.2
		III	−0.09	0.2	0.18	−0.02	−0.27	−0.07	−2.28	1.76	1.49
		IV	−0.23	0.41	0.37	0.13	−0.6	0.27	−1.44	3.12	5.55
144	0.8	I	0.08	0.11	0.12	0.07	−0.05	−0.02	−0.24	0.31	−1.0
		II	0.08	0.09	0.13	0.13	−0.05	0.01	−0.67	0.83	−0.52
		III	−0.11	0.28	0.43	0.40	−0.5	0	−0.84	0.95	0.34
		IV	−0.22	0.32	0.77	0.39	−0.99	−0.06	−0.1	2.2	4.1
117	0.7	I	0.11	0.09	0.50	0.42	−0.36	−0.32	0.1	0.1	−0.82
		II	0.08	0.08	0.5	0.45	−0.42	−0.33	0.06	0.13	−1.01
		III	0.05	0.14	1.07	0.68	−1.08	−0.55	0.14	0.35	−0.55
		IV	−0.04	0.01	1.48	0.89	−1.58	−0.61	0.55	0.79	2.71

Errors were calculated as values estimated from the simulation input values. Splittings were determined from simulated spectra for different conformations, without added noise. The digital resolution was 4.8 Hz/point in F1 and 0.78 Hz/point in F2. Errors are reported as the difference between the measured value and the known input value. Pairs of values are for measurements made from different cross-peaks, parallel to the F2 axis.

[a] LW refers to different sets of line widths (in Hz), as follows: (I) H1' = 3.5, H2' = 7.5, H2" = 7.5, H3' = 3.8, H4' = 4.4; (II) H1' = 3.6, H2' = 9.6, H2" = 8.4, H3' = H4' = 4.2; (III) H1' = 5.5, H2' = 11.2, H2" = 11.7, H3' = H4' = 4.8; and (IV) H1' = 6.5, H2' = 22, H" = 22, H3' = 5.8, H4' = 6.1.

TABLE 4
ANALYSIS OF SUGAR CONFORMATIONS USING PFIT WITH SIMULATED DATA

Data set	P_S (°)		f_S	
	Mean	Range	Mean	Range
i	156 ± 10	142–173	0.83 ± 0.03	0.81–0.9
ii	151 ± 12	131–170	0.82 ± 0.036	0.78–0.90
iii	166 ± 9	159–177	0.78 ± 0.07	0.69–0.9
iv		95–195		0.75–0.9

Sugar conformations were analysed by fine-grid searching, as described in the Methods. Data sets consisted of: (i) 10 runs with $\sum_{1'}$ in the range 14.0 to 14.7 Hz, $\sum_{2'}$ 28.2 to 30.0 Hz and $\sum_{1''}$ 21 to 23 Hz; (ii) sums of coupling constants as for dataset i plus the H1'-H4' distance in the range 0.28 to 0.35 nm and the H2"-H4' distance 0.32 to 0.4 nm; (iii) $\sum_{1'}$ in the range 13.7 to 15.0 Hz plus the two distance ranges; and (iv) $\sum_{1'}$ in the range 14 to 14.5 Hz only. The mean values were calculated with the best (i.e., lowest residual) error for each run.

spin-echo methods. It also tends to suppress effects of exchange processes on the relaxation rate. Table 1 shows $R_{1\rho}$ values, measured where possible from the one-dimensional rotating-frame experiments (see Methods) at different temperatures. Because R_2 is dominated by J(0) for macromolecules, it is expected to vary according to the Stokes–Einstein relationship (Lane et al., 1986). The correlation time for the C H6-H5 vectors is expected to vary approximately twofold between 25 °C and 50 °C. Within experimental error, the R_2 values in Table 1 are in agreement with this expectation. The line widths of proton resonances that are resolved in one-dimensional spectra were determined by line-shape fitting using routines in the Varian VNMR software, and the contribution from residual magnetic field inhomogeneity was accounted for by subtracting the line width of the CH_3 resonance of DSS. R_2 values estimated from the experimental line widths and those measured as $R_{1\rho}$ agreed within 5% both for base protons and H1'. This good agreement justifies the use of the rotating-frame experiment to estimate line widths.

Because of the extensive spectral overlap, the one-dimensional method is not suitable to measure the line width of most sugar protons. We have therefore developed a two-dimensional method for measuring $R_{1\rho}$ (see Table 2). The data obtained from the 1D and 2D rotating-frame T_1 experiments, under the same conditions, are in excellent agreement with each other. In most cases the $R_{1\rho}$ value determined from the 2D experiment for a certain proton is slightly higher than the value obtained from the 1D experiment. A possible explanation for this behaviour could be the poorer signal-to-noise ratio in the 2D spectra, leading to a systematic underestimation of the signal at long delay times.

The $R_{1\rho}$ values of protons on terminal residues are typically ca. twofold smaller than those in internal residues, in part reflecting the smaller number of nearest neighbours. However, the rigid-body calculation (see above) suggests that a smaller number of nearest neighbours should decrease the relaxation rate constants by a considerably smaller factor. Moreover, ^1H and ^{13}C relaxation measurements have shown (Lane, 1991; Borer et al., 1994) that order parameters for spins in terminal residues can be two- to threefold smaller than in internal residues, indicating substantial mobility on the subnanosecond time scale. The terminal residues of the hexadecamer are therefore probably more mobile than the internal residues. The difference between the relaxation rates for purine H8 and pyrimidine H6 can be in part attributed to the H5 or Me neighbour of the H6, which would contribute 2.5 to 3 s^{-1} to $R_{1\rho}$. For both H1' and H2", the relaxation rates are significantly larger in purines than in pyrimidines, on average, whereas there is no such difference on average for H2' or H3'. However, there are substantial individual variations in the relaxation rates for a given type of proton, which may reflect sequence-dependent differences in conformation. These results quite clearly demonstrate that a unique line width cannot be assigned to a particular proton type, which has important consequences for the analysis of coupling constants based on simulations (see below).

Effect of line width, digital resolution and noise on splittings in COSY spectra

Although simulations of cross-peaks in DQF-COSY (Gochin et al., 1990; Schmitz et al., 1990,1992; Majumdar and Hosur, 1992) and P.COSY (Macaya et al., 1992) have been published, a systematic evaluation of the cross-peak fine structure as a function of line widths, digiti-

TABLE 5
ANALYSIS OF SUGAR CONFORMATIONS USING SIMULATED COUPLING CONSTANTS AND NOEs

Data set	P (°)	f	$-\chi$ (°)
i	144–162	0.75–0.85	105–110
ii	126–162	0.75–0.85	108–112
iii	130–198	0.7–0.8	103–108
iv	90–198	0.7–0.9	108–113
v	126–198	0.75–0.85	102–113
vi	90–198	0.8–0.9	110–115

NOEs and coupling constants for a three-base-pair fragment of DNA, d(CGA)·d(TCG), were calculated using the program NUCFIT (Lane, 1990). The DNA fragment was in the B-form, except for G2, for which the nucleotide was described by $\chi(S) = -110°$, $P_S = 144°$, $f_S = 0.8$, $\phi_m = 36$, $P_N = 9°$ and $\chi(N) = -150°$. NOESY time courses were generated for a spectrometer frequency of 500 MHz and an isotropic rotational correlation time of 3 ns, using D_2O as the solvent. Errors in the NOE intensities were set at ±15%. The range of solutions is given for which the mean residual error, R, is less than 0.15. The data sets used were the following: (i) $\sum_{1'}$ (± 1 Hz), $\sum_{2'}$ (± 2 Hz) and $\sum_{2'}$ (± 2 Hz), NOEs from G H8 to G H1', H2', H2" and H3' and G H4' to H1' and H2", using time points at 50, 100, 150, 200 and 300 ms; (ii) coupling constants as above, and NOEs for G H8 to the sugar protons only; (iii) all NOEs and no coupling constants; (iv) NOEs for G H8 to sugar protons only; (v) all NOEs + $\sum_{1'}$ only; and (vi) G H8–sugar proton NOEs and $\sum_{1'}$.

sation and noise for long correlation times has not been previously shown. We have simulated DQF-COSY and P.E.COSY spectra for a complete deoxyribose spin system using the program Gamma (Smith et al., 1994), in which the digital resolution and the line widths for different conformations were systematically varied. The influence of line width was simulated using digital resolutions corresponding to those actually obtained in our experiments (see above).

Figure 1 shows the effect of varying the line widths on the H2'-H1' and H2"-H1' cross-peaks, and also on the H2'-H3' cross-peak. The H1'-H2' cross-peaks (Fig. 1A) change radically as the line width is increased for a fixed conformation analogous to the experimental data (see below). However, remarkably similar cross-peak patterns can be obtained for different conformations if the line widths are also altered. For example, the H2'-H1' DQF-COSY cross-peak appears very similar for the conformations $P_S = 162°$, $f_S = 0.8$ ($^3J_{1'2'} = 8.6$, $^3J_{1'2''} = 5.7$ Hz) and $P_S = 117°$, $f_S = 1.0$ ($^3J_{1'2'} = 10.2$, $^3J_{1'2''} = 5.5$ Hz) if different line widths are chosen (Fig. 1D). Similarly, the H3'-H2' cross-peaks appear very similar for $P_S = 144°$, $f_S = 0.8$ ($^3J_{1'2'} = 8.8$, $^3J_{1'2''} = 2.5$ Hz) and $P_S = 180°$, $f_S = 1.0$ ($^3J_{1'2'} = 9.8$, $^3J_{1'2''} = 0.9$ Hz) for different line widths (Fig. 1C). This suggests that accurate J-values cannot always be obtained by simulation.

With simulated data, it is possible to measure the error of the apparent coupling constants derived from such spectra. Table 3 shows typical errors for coupling constants (or sums of coupling constants) measured from simulated DQF-COSY spectra under conditions of no noise and good digital resolution (i.e., ideal spectroscopic conditions). Four sets of line widths are shown, corresponding to those expected or measured at 50 °C ($\tau = 2.8$ ns, set I), 40 °C ($\tau = 3.6$ ns, sets II,III) and 25 °C ($\tau = 6.1$ ns, set IV) for the hexadecamer studied here. As expected, the errors for the coupling constants are the smallest for the narrowest lines, generally < 0.5 Hz, and even in the worst case, they are not more than 1 Hz. As the line widths are increased, the errors also increase, such that for the largest line widths, the errors in some parameters (particularly $\Sigma_{2''}$ and to a lesser extent $\Sigma_{2'}$) are so large as to render them useless for conformational analysis. Nevertheless, the value of $\Sigma_{1'}$ is still quite well determined even for the broadest lines. This is probably because H1' is intrinsically quite narrow (the estimated line width at 25 °C is ca. 6.5 Hz), and therefore smaller than the active couplings. The determination of the individual couplings to H1' are also poor at larger line widths, and rather accurate values are needed if these are to be used to define the sugar conformation (Van Wijk et al., 1992).

Whilst the variation of the splitting for an antiphase doublet of Lorentzian lines has been investigated as a function of the digital resolution and line width (Neuhaus et al., 1985; Wüthrich, 1986; Majumdar and Hosur, 1992), the situation is more complex for multiplets with more

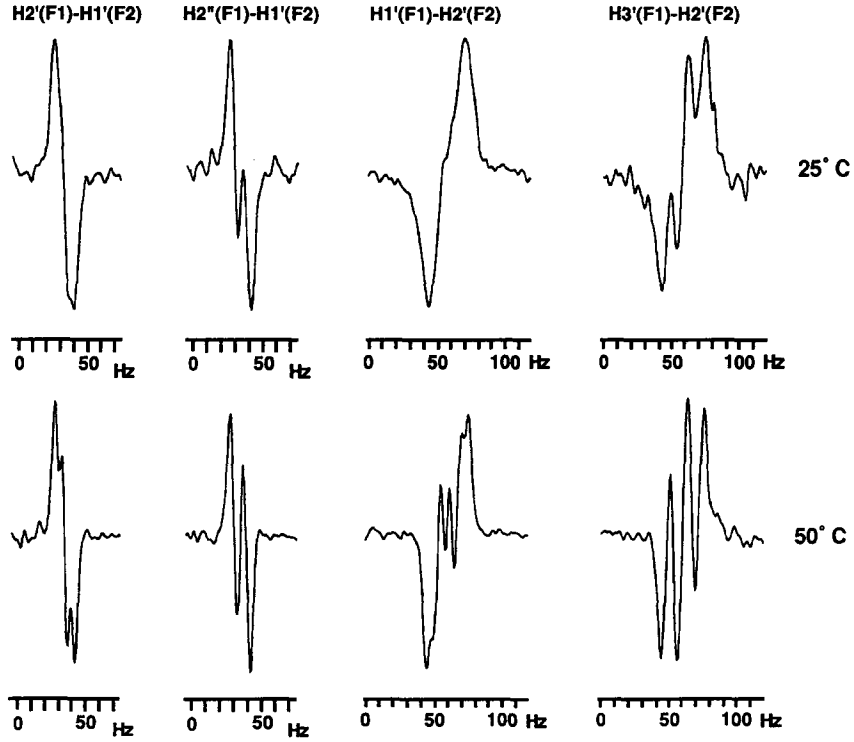

Fig. 3. Cross sections through T5 H1' and T3 H2' from DQF-COSY spectra of d(CATGTGACGTCACATG)$_2$. Spectra were recorded and processed as described in the Methods. Peaks have all been scaled to the same height and the noise for the H2"-H1' peaks appears substantially higher than for the H2'-H1' peaks, and similarly for the H3'-H2' and H1'-H2' cross-peaks. The cross sections are shown in pairs, at 25 °C (upper) and 50 °C (lower). The cross sections shown are (left to right): T5 H2'-H1', T5 H2"-H1', T3 H1'-H2' and T3 H3'-H2'.

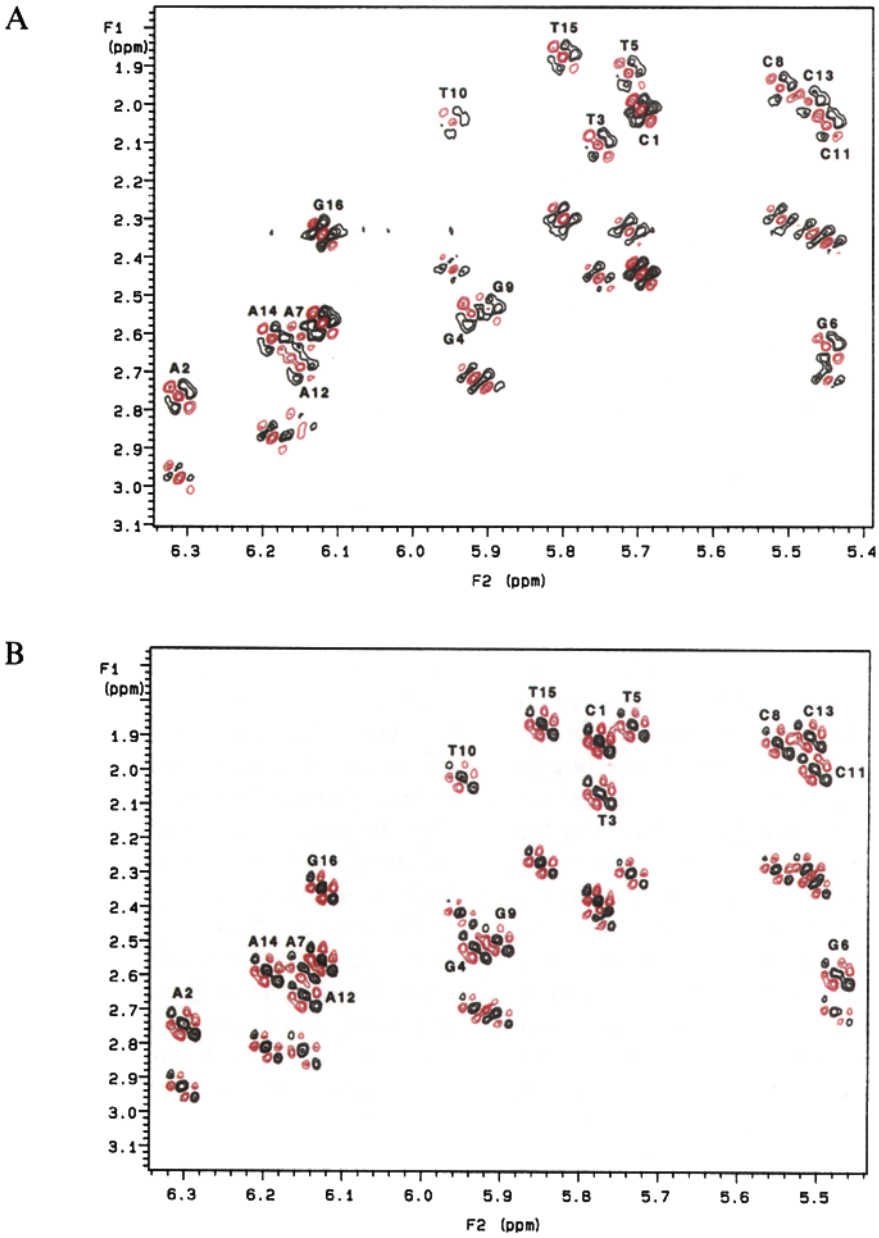

Fig. 4. Experimental P.E.COSY spectra of d(CATGTGACGTCACATG)$_2$. The spectra were at 11.75 T recorded at 25 °C and 50 °C, as described in the Methods. The data matrices consisted of 8192 complex points in t_2 and 2048 complex points in t_1, to give final digital resolutions of 1.22 and 4.88 Hz/point in F2 and F1, respectively. The free induction decays were multiplied by shifted Gaussian functions in both dimensions. (A) Spectrum at 25 °C; and (B) spectrum at 50 °C.

than one splitting, such as H2'-H1' and H2"-H1'. For a sugar in an S-type conformation, the H2"-H1' cross-peak shows a +−+− pattern along F2. The inner two antiphase lines generally have a small separation, so that for broad peaks these tend to cancel, and the separation between the outer peaks (i.e., $\sum_{1'}$) is overestimated. By contrast, the H2'-H1' cross-peak shows a ++−− pattern along F2, which for broad lines leads to coalescence of the two positive peaks and of the two negative peaks, resulting in a net separation that underestimates $\sum_{1'}$. The important parameter then is the separation between multiplet components, and their relationship to the line width. Upper and lower limits to the value of $\sum_{1'}$ can be estimated if the separations can be measured in both cross-peaks. Similar considerations apply to $\sum_{2'}$. For broad resonances, which is especially true of H2' and H2", the H1'-H2' cross-peak shows a ++−+−+−− pattern along F2. The inner antiphase lines tend to cancel, whereas the outer pair of in-phase lines tend to amalgamate, leading to an estimate of $\sum_{2'}$ that is too small. Because H2' is always much broader than H1' (cf. Tables 1 and 2), this will be a much more serious problem for $\sum_{2'}$ than for $\sum_{1'}$. The alternative cross-peak for $\sum_{2'}$ is H3'-H2'. In the F2 dimension, the active H2'-H3' coupling is ca. 6–8 Hz, and the

passive couplings (for an S-type conformation) to H2" and H1' produce a fine structure +−++−−+−. The inner components tend to cancel, leaving the outer peaks which slightly overestimate $\sum_{2'}$.

The relationship between line width and apparent splittings is obviously dependent on the antiphase character of the cross-peaks in COSY experiments. In principle, cross sections through NOESY peaks should provide the same information, but will appear different because all of the components of the multiplets are in-phase. Naturally, this always leads to coalescence of peaks when the frequency differences are smaller than the line widths, and therefore the measured splittings can provide a lower limit to coupling constants. Extensive simulations (data not shown) indicate that only $\sum_{1'}$ can be obtained with any reliability when the line widths become large. The coalescence of the many components for $\sum_{2'}$ completely destroys the resolution, and it becomes impossible to distinguish components to measure a splitting.

Another important parameter that affects the appearance of the cross-peak patterns is digital resolution. We have systematically examined the effect of resolution on the DQF-COSY cross-peaks for two different sets of line widths, corresponding to $\tau = 2.8$ ns and $\tau = 3.6$ ns. In general, the effect of poorer resolution is the greatest for individual coupling constants and $\sum_{2'}$ or $\sum_{2''}$, and the least for $\sum_{1'}$. For the latter sum, the error is small (< 0.5 Hz) at a digital resolution of 1 Hz per point or better. This error increases as the resolution worsens, and under the worst conditions, $\sum_{1'}$ may be in error by more than 2 Hz (2 Hz per point in F2). Note that this is for noise-free data with relatively narrow line widths. Resolutions poorer than ca. 1.5 Hz/point in F2 are likely to give substantial errors in most coupling constants, indicating that long acquisition times in t_2 should be used for such spectra.

P.E.COSY (Mueller, 1987; Bax and Lerner, 1988) is an alternative to DQF-COSY in that it reduces the number of components in the cross-peaks, and therefore in principle makes the analysis simpler. The H2'-H1' and H2"-H1' cross-peaks consist of two resolved parts in F1, because of the relatively large passive geminal coupling, $^2J_{2'-2''} \approx -14$ Hz, and two quite resolved parts in F2, which correspond to the characteristic pattern for S-type sugars ($J_{1'-2'} > J_{1'-2''}$) (see below). We have simulated the effects of digitisation and line width on P.E.COSY cross-peaks. Again, to recover accurate coupling constants, rather good digital resolution is essential (i.e., ≤ 1.5 Hz/point in F2). With increasing line width, it becomes impossible to determine the offset between the two parts of the cross-peak, and indeed, the shape of the cross-peaks depends critically on digitisation and the weighting function used for processing: the same data with different weighting functions can produce remarkably different cross-peak patterns (data not shown). The error is very dependent on digitisation, line width and the method of data processing. Furthermore, there are no obvious trends in the error as a function of conformation. Hence, the determination of $^3J_{1'2'}$ and $^3J_{1'2''}$, $\sum_{2'}$ and $\sum_{2''}$ are unlikely to be very accurate for larger oligonucleotides under realistic experimental conditions. In addition, Norwood (1995) has shown that measurements of coupling constants from E.COSY spectra of large molecules are likely to be in error because of cross-relaxation effects.

The third consideration that affects the measurement of accurate coupling constants is the signal-to-noise ratio. Simulations with Gaussian noise added to spectra showed that, where the line width and digitisation were sufficient to provide useful cross-peaks, addition of noise severely degraded the estimates, rendering them useless for conformational analysis. For example, cross sections through H1'-H2'/H2" for the larger line widths can yield some useful information in the absence of noise. The value of $\sum_{1'}$ is the least affected by noise. Our simulations show that even when the signal-to-noise ratio in a cross section is as low as 3:1, the $\sum_{1'}$ can be determined to within about 0.4 Hz for narrow lines. However, for the broader resonances at long correlation times, the error can increase to nearly 1 Hz at this level of noise. Values of $\sum_{2'}$ are grossly distorted when the signal-to-noise ratio is ca. 5:1 or less, even for the spectra recorded with narrow lines (data not shown). As larger molecules tend to have lower sensitivities in terms of peak height, the effect of noise is likely to be substantial.

The combined influence of line widths and noise for larger oligonucleotides suggests that the most reliable scalar information is $\sum_{1''}$, and in many instances, only inaccurate values can be obtained for other coupling constants. As $\sum_{1'}$ alone provides little information about conformation (though is a good indicator of f_S), it is clear that additional information is needed to determine sugar conformations in larger nucleic acid fragments. We have therefore evaluated the use of NOEs or distances derived from NOEs in conjunction with measurable coupling constants for estimating sugar conformations.

Analysis of P_S and f_S with and without distances

Coupling constants and distances for H1'-H4' and H2"-H4' were generated for a deoxyribose having $P_S = 144°$, $\phi_m = 36°$, $f_S = 0.8$ and $P_N = 9°$. Various sets of the sums of coupling constants were generated and used as input to the program PFIT. The program was run using values of P_S ranging from 90° to 198° and f_S from 0.5 to 1 in intervals of 4° and 0.03, respectively. When used, the upper and lower distance bounds were set to 0.35 and 0.28 nm for H1'-H4' and 0.4 and 0.32 nm for H2"-H4'. Table 4 shows results of the simulations, where the best values correspond to those for which the residual error R(J) was a minimum, and the range was for parameters for which the residual error was < 2%. Using input values without error for the coupling constants, the program recovered

the correct values (data not shown). When typical experimental errors were added to the target coupling constants, the mean value of P_S was found to be $156° \pm 10°$ (range 142°–173°) and $f_S = 0.83 \pm 0.03$ (range 0.81–0.9) in the absence of distance constraints. In this case, adding the distance constraints had an insignificant effect on the result (Table 4). If only $\sum_{1'}$ and the distance constraints were used, the value of P_S was found to be $166° \pm 9°$ (range 159°–177°) and $f_S = 0.78 \pm 0.07$ (range 0.69–0.9). These results indicate that if three coupling constants (or sums of coupling constants) can be determined with reasonable precision, the value of P_S will be constrained within a range of about 30°, and f_S within an interval of around 0.1. In this instance, adding the distance constraints does not have much influence. Much tighter distance intervals would be needed to improve the determination of the sugar conformation, but the uncertainties arising from spin diffusion and internal motions would make this difficult. However, if only $\sum_{1'}$ is available with reasonable precision (±0.5 Hz), such as for slowly tumbling macromolecules, then adding distance constraints significantly improves the determination of the sugar conformation, although P_S may be overestimated. It should be noted that for a mixture of conformations, the value of $\sum_{1'}$ alone would not constrain P_S to better than ca. 90°–198°.

Analysis using NOE time courses and coupling constants

Direct analysis of NOE time courses employs all of the experimental data, and allows modelling of conformational equilibria in a simple fashion, leading to better determination of the most sensitive conformational parameters (Lane, 1990). We have simulated NOESY time courses for the three-base-pair fragment d(CGA)·d(TCG).

The values of χ(S), P_S and f_S for G2 were varied systematically, with nonlinear optimisation of χ(S) for four versions of the data set, as shown in Table 5. The minimal data set iv gave good values of χ, as expected, but the residual R was essentially the same for P_S over the entire range from 126° to 180°, and f_S was found to be ca. 0.7. As previously reported (Lane, 1990), these NOEs do not fix P_S precisely within the S domain. Using all NOEs, but no coupling constants (data set iii) gives a narrow range for P_S, a good value of χ(S) and a reasonable estimate of f_S. Data set ii similarly gives a better determination of both P_S and f_S, whereas the complete set of data, as expected, performs best of all with rather precise estimates of χ, P_S and f_S. However, for large nucleic acids, it is probable that only $\sum_{1'}$ can be reliably measured with reasonable accuracy, which in itself provides information only about f_S in the range $90° < P_S < 180°$. In larger oligonucleotides, such as DNA triplexes, spectral resolution may allow only a subset of the intranucleotide NOEs to be measured. If only $\sum_{1'}$ is available, and all intranucleotide NOEs can be measured, then the determination of P_S and f_S is quite good. If the intrasugar NOEs are not measurable, and only $\sum_{1'}$ is available, then P_S is not well determined (the error function is only weakly dependent on P in the range 90° to 180°).

Analysis of sugar conformations in the hexadecamer

Scalar couplings in d(CATGTGACGTCACATG)$_2$

The nonexchangeable protons of the hexadecamer have been assigned by standard methods (M.R. Conte and A.N. Lane, unpublished data), and will be reported elsewhere. Figure 2 shows DQF-COSY spectra of the H1'/H3' to H2'/H2" region at 25 °C and 50 °C. The spectra clearly show the extra fine structure present at the higher temperature (cf. the cross-peaks for T3 and A2). Furthermore, the H3'-H2' cross-peaks are more numerous or more intense at the higher temperature and also display much more detail. As we will show below, this improvement in resolution is largely a consequence of the smaller line width at 50 °C. The details of the fine structure, the lack of H3'-H2" cross-peaks and the measured value of $\sum_{1'}$ ($= {}^3J_{1'2'} + {}^3J_{1'2''}$) is indicative of sugars in the S domain.

The details of the fine structure can be seen more readily in cross sections. Figure 3 shows cross sections of the DQF-COSY spectra through different cross-peaks of the protons T5 H1' and T3 H2' at 25 °C and 50 °C. At 50 °C, the fine structure is resolved in F2 for all of the cross-peaks, showing the expected four-line patterns for coupling to H1', and the eight-line pattern for H1'-H2'. Accidental cancellation occurs between close antiphase components in the H3'-H2' cross-peaks, even at 50 °C. However, at 25 °C the fine structure has largely or completely disappeared as a consequence of the increased line widths. This results in significant errors in the estimation of $\sum_{1'}$, and ${}^3J_{1'2'}$ and ${}^3J_{1'2''}$ cannot be determined from such spectra. The effect of line width is more pronounced for the H1'-H2' and H3'-H2' cross-peaks. At 25 °C, there is no fine structure in the H1'-H2' cross-peak, and $\sum_{2'}$ ($= {}^3J_{2'1'} + {}^3J_{2'3'} + {}^2J_{2'2''}$) is substantially underestimated from the separation between the extrema compared with the results for higher temperatures. Also, as expected, the signal-to-noise ratio (considered as peak height) is much poorer at 25 °C than at 50 °C, again as a consequence of the relative line widths.

Table 6 presents the apparent splittings obtained from DQF-COSY and NOESY spectra recorded at two temperatures. As the temperature is increased, the estimate of $\sum_{1'}$ averaged from the H2'-H1' and H2"-H1' splittings in both experiments increases, and in general the splitting measured in the DQF-COSY experiment is larger than that measured from NOESY data. This is as expected from the influence of line widths on antiphase and in-phase cross-peaks. Similarly, the estimate of $\sum_{2'}$ increases as the temperature is increased, whereas that of $\sum_{2''}$ ($= {}^3J_{2''1'} + {}^3J_{2''3'} + {}^2J_{2'2''}$) decreases with increasing tem-

TABLE 6
MEASURED SPLITTINGS AND DISTANCES FOR PROTONS OF d(CATGTGACGTCACATG)$_2$

Nucleotide	$\Sigma_{1'}$ (Hz)		$\Sigma_{2'}$ (Hz)		$\Sigma_{2''}$ (Hz)		$I_{3'4'}$	$r_{1'-4'}$ (nm)		$r_{2''-4'}$ (nm)	
	25 °C	50 °C	25 °C	50°C	25 °C	50 °C		25 °C	50 °C	25 °C	50 °C
C1	13.8	14.1	28.2	28.4	21.5	nd[a]	s	0.303	0.306	0.31	0.33
	13.5	14.1	27.5	28.0	nd	nd					
A2	14.6	15.1	29.7	28.6	22.5	21.2	m	0.30	0.306	0.34	0.35
	13.9	14.6	nd	29.3	nd	19.5					
T3	14.6	15.1	26.8	29.9	26	24.2	s (4.8)	0.29	0.283	0.33	0.345
	14.2	14.6	nd	31	nd	nd					
G4	nd	14.8	nd	28.8	nd	22.0	m (4.2)	0.293	0.298	0.35	0.35
	nd	nd	nd	nd	nd	nd					
T5	15.3	15.2	28.9	30	24.3	22.2	m	0.286	0.286	nd	nd
	14.6	15.1	nd	nd	nd	21.1					
G6	nd	15.2	24.4	26.2	25.9	21.2	w	0.29	0.294	nd	nd
	14.8	15.0	nd	nd	nd	19.7					
A7	nd	15.4	nd	nd	nd	nd	w	0.298	0.297	0.35	0.34
	nd	nd	nd	nd	nd	nd					
C8	14.4	14.7	27.5	29	25.5	21.9	m/s	0.28	0.284	nd	nd
	13.0	14.5	29.5	nd	nd	nd					
G9	nd	14.7	nd	28	nd	22.7	m (4.6)	0.291	0.298	nd	nd
	nd	nd	nd	nd	nd	nd					
T10	15.3	15.4	26.4	30	26.4	22.9	m	nd	0.28	0.35	0.345
	nd	15.2	nd	nd	nd	20.4					
C11	nd	14.7	27	28.6	23.6	nd	nd	0.29	0.298	0.34	nd
	nd	14.6	nd	nd	nd	nd					
A12	nd	15.2	26	28.5	nd	nd	w	0.295	0.297	0.35	0.36
	nd	14.9	nd	28.9	nd	nd					
C13	nd	4.8	nd	29.2	nd	nd	m/s	nd	nd	0.32	nd
	nd	14.9	nd	29.1	nd	nd					
A14	14.4	14.7	26.3	27.4	25.2	21.9	nd	0.295	0.297	0.35	0.36
	13.9	14.5	nd	29.8	nd	nd					
T15	14.9	15.1	28.8	30.1	24	22.2	m/s	0.277	0.277	nd	nd
	14.6	14.9	nd	30.7	nd	19.7					
G16	14.4	14.4	28.4	28.2	23.3	22.1	s (3.7)	0.315	0.323	0.34	0.34
	14.2	14.4	27	nd	23.2	22.7					

Splittings were determined from DQF-COSY and NOESY spectra, as described in the text. The first value was obtained with DQF-COSY; the second one with NOESY. Presented values of $\Sigma_{1'}$ from DQF-COSY are the averages of the H2'-H1' and H2''-H1' cross-peaks (values from only one splitting are not given); values of $\Sigma_{2'}$ from DQF-COSY are the averages from the H1'-H2' and H3'-H2' cross-peaks, except for G6 where only the value from H1'-H2' was measured; $I_{3'4'}$ denotes the intensity (strong, medium or weak) of the H3'-H4' cross-peak in DQF-COSY; the value in parentheses is the coupling constant estimated from the J-scaled DQF-COSY experiment, as described in the text; $r_{1'4'}$ and $r_{2''4'}$ are the distances between H4' and H1' and H2'', determined as described in the text. Errors are estimated to be (at 25 °C and 50 °C, respectively): ± 1/1.5 Hz and ±0.5 Hz for $\Sigma_{1'}$; ± 2/2.5 Hz and ± 1 Hz for $\Sigma_{2'}$, except for A2, A12 and A14 (± 4 and ± 2 Hz), for G4 and G9 (± 5 and ± 2.5 Hz) and for G6 (± 6 and ± 3 Hz); ± 4 Hz and ± 2 Hz for $\Sigma_{2''}$.

[a] nd = not determined.

perature. The difference between the estimates at 25 °C and 50 °C can be large (> 2 Hz), especially for $\Sigma_{2''}$. In most instances, the line widths were too large to resolve fine structure in the cross-peaks in the NOESY experiment, so that the coupling constants could not be estimated reliably.

The experimental splittings in DQF-COSY spectra depend strongly on the temperature (cf. Table 6). The simulations based on measured line widths showed that the primary cause of the differences is the relative size of the line widths compared with the coupling constants. This is shown further by the observation that the value of $\Sigma_{1'}$ measured from the H2'-H1' cross-peak agrees with the value measured from the H2''-H1 cross-peak to within 0.5 Hz only for the data acquired at 50 °C, where H1' line widths are ca. 3 Hz. For larger line widths, at 25 °C H2'-H1' and H2''-H1' splittings appear to be under- and over-estimated respectively, as shown in the simulation. Furthermore, the values of $J_{1'2'}$ and $J_{1'2''}$ are not at all well determined at 25 °C. It was impossible to determine either $\Sigma_{2'}$ or $\Sigma_{2''}$ at 25 °C, and $\Sigma_{1'}$ could be established only for a few residues (including the terminal nucleotides) if the spectra were subjected to strong resolution enhancement. In the absence of other information, sugar puckers cannot be determined at the lowest measured temperature using COSY data alone.

TABLE 7
CONFORMATIONAL DATA OF d(CATGTGACGTCACATG)$_2$ AT 50 °C

Nucleotide	f_{S1}	P_{S1} (°)	P_{S2} (°)	f_{S2}
C1	0.65–0.75	153	160 (–5/+5)	0.73
A2	0.81–0.95	153	160 (–10/+10)	0.88
T3	0.81–0.92	130	158 (–7/+12)	0.88
G4	0.81–0.92	144	166 (–6/+5)	0.85
T5	0.84–0.95	130	149 (–9/+5)	0.91
G6	0.86–0.98	142	155 (–5/+5)	0.92
A7	0.84–0.95	150	171 (–30/+10)	0.88
C8	0.75–0.87	130	145 (–5/+20)	0.85
G9	0.81–0.92	144	141 (–5/+5)	0.9
T10	0.87–0.98	126	149 (–5/+10)	0.94
C11	0.82–0.87	144	176 (–20/+1)	0.85
A12	0.86–0.97	150	170 (–10/+10)	0.93
C13	0.78–0.89	144	160 (–5/+10)	0.85
A14	0.78–0.89	150	166 (–20/+20)	0.85
T15	0.84–0.92	126	154 (–8/+8)	0.89
G16	0.78–0.84	162	176 (–20/+4)	0.79
Mean ± sd				
R	0.88 ± 0.03	148 ± 4	161 ± 10	0.88 ± 0.03
Y	0.86 ± 0.04	131 ± 6	156 ± 9	0.88 ± 0.03

Coupling constants and distances were measured at 50 °C as described in the text; f_{S1} was calculated from $\Sigma_{1'}$ according to Eq. 5. P_{S1} was calculated as described by Van Wijk et al. (1992); calculations with PFIT were done as a grid search over 200 conformations with coupling constants set to the center of the range, as reported in Table 6; distances were taken from Table 6. P_{S2} and f_{S2} are the best-fit values and the range (in parentheses) denotes fits for which the residual error was twice that of the minimum error.

As the line width has the largest effect on the DQF-COSY spectra, and the agreement between coupling constants estimated from different cross-peaks is acceptable at 50 °C, we will use these data to determine the sugar conformations. We assume that the conformations of the sugars are not significantly temperature-dependent, as was found by Rinkel et al. (1987), and is supported in the present study by the H1'-H4' and H2"-H4' NOEs measured at different temperatures (Table 6, and see below).

The values of all of the coupling constants, the details of the fine structure of the DQF-COSY and the values of the distances in Table 6 are not consistent with any unique conformation. It is therefore necessary to consider a conformational mixture of N and S states.

Because the value of $\Sigma_{1'}$ varies less than 1 Hz over the range $80° < P < 180°$, it provides a means of estimating the fraction of the S-type conformer (Rinkel and Altona, 1987; Van Wijk et al., 1992):

$$f_S = (\Sigma_{1'} - 9.8) / 6.3 \quad (5)$$

$\Sigma_{1'}$ values were measured from resolution-enhanced 1D spectra where possible and from H2'-H1' and H2"-H1' cross sections of phase-sensitive DQF-COSY and NOESY spectra, in order to take into account the errors of the apparent outer peak separation obtained from both in-phase and antiphase experiments (see above). Even at 50 °C, the values of $\Sigma_{1'}$ estimated from NOESY spectra are smaller than those estimated from the DQF-COSY spectrum. The best values of $\Sigma_{1'}$ as averages from H2'-H1' and H2"-H1' splittings, as determined by our experiments at 50 °C, are given in Table 6. A similar procedure was applied to estimates of $\Sigma_{2'}$, using the H1'-H2' and H3'-H2' DQF-COSY and NOESY cross-peaks (Table 6). For all of the pyrimidine and also the terminal nucleotides it was possible to obtain an agreement between the apparent $\Sigma_{2'}$ couplings measured in all experiments at 50 °C within 1–2 Hz. By contrast, for the purines the $\Sigma_{2'}$ couplings measured from DQF-COSY H2'-H1' cross sections appear to be underestimated even at 50 °C, whereas those obtained from H2'-H3' cross sections are overestimated compared to the values determined from the other experiments. Hence, in the sugar analysis (see also below) for A2, A12 and A14, $\Sigma_{2'}$ was taken only from the apparent couplings of NOESY spectra, and therefore does not have the same statistical significance as those for other nucleotides. For G4 and G9, no apparent $\Sigma_{2'}$ couplings were determined from NOESY spectra, so that a large range of $\Sigma_{2'}$ was found (± 3 Hz), based on the values obtained from H1'-H2' and H3'-H2' DQF-COSY cross sections, respectively. For G6 it is possible to define only the lower limit of this range, since the apparent $\Sigma_{2'}$ from the H3'-H2' cross section was not determined.

The value of f_S was calculated for each nucleotide from $\Sigma_{1'}$ (Van Wijk et al., 1992), and an estimate of P_S from $\Sigma_{2'}$, where possible. Values of P_S estimated in this manner will be denoted P_{S1} (Table 7). The last two columns of Table 7 show the best estimates of f_S and P_S using the program PFIT (denoted f_{S2} and P_{S2}, respectively), including distances given as ranges –100/+50 pm for H1'-H4', and –50/+50 pm for H2"/H4'. The values of P_S and f_S presented in Table 7 were calculated assuming that $\phi_m = 36°$. Additional calculations (data not shown) for $\phi_m = 28°$ and 44° changed the estimate of P_S by $< 10°$.

The sugar conformations were confirmed by estimation of the H1'-H4' distance ($r_{1'4'}$), which is sensitive to the pseudorotation phase angles, and the H2"-H4' distance ($r_{2''4'}$), which depends predominantly on the fraction of molecules in the S state (Van de Ven and Hilbers, 1988; Conte et al., 1995). Table 6 shows distances for each nucleotide at 50 °C determined as described in the Methods. In addition, we report the relative intensities of the H3'-H4' DQF-COSY cross-peaks. As the line width of H3' and H4' seems not to vary much from one residue to another (cf. Table 2), except for the terminal ones (Table 2 and below), these latter relative intensities are proportional to the value of $^3J_{3'4'}$ (Searle, 1993; Conte et al., 1995) which depends on both P_S and f_S. We tried to measure the $^3J_{3'4'}$ coupling directly from a partially decoupled J-scaled DQF-COSY experiment developed by Bax and

Lerner (1988). Because of the severe overlap of H3' and H4' resonances of the pyrimidines, and the extreme weakness of the H3'-H4' cross-peak for A2, A12, A7 or its absence for G6, even at 50 °C, it was possible to determine only a few $^3J_{3'4'}$ values (Table 6), which, however, appear to be overestimated (by 0.5–1.5 Hz) probably because under these conditions line widths are larger than couplings.

The sums of the coupling constants and the two distances were used for simultaneous fitting with PFIT, as shown in Table 7. In general, the value of P_{S2} found when including the distance data is larger than that obtained when just using the coupling constants alone, though the relative variation from one nucleotide to the next is preserved. This suggests that the true precision of the determination of P_S is around ±20°. It is also possible that the distances have a systematic bias from effects of spin diffusion and internal motion that is not modelled by this approach (see below). In neither analysis is there a significant difference in f_S for purines and pyrimidines, but there may be a (slight) tendency for P_S of purines to be larger than P_S of pyrimidines.

Coupling constants from P.E.COSY

In order to obtain additional information about the sugar conformation of the hexadecamer as well as to determine whether other 2D NMR techniques are more suitable to determine coupling constants in large DNA fragments, $^3J_{1'2'}$ and $^3J_{1'2''}$ have been estimated from P.E.COSY spectra (Mueller, 1987; Bax and Lerner, 1988) at 50 °C (see above). The H1'-H2' and H1'-H2" cross-peaks show slight differences among the various nucleotides (Fig. 4), indicating variations in P_S (or f_S). It is clear that, whilst the splittings corresponding to the two coupling constants can be readily estimated from the spectrum recorded at 50 °C, it is much more difficult to decide where to do the measurement in the spectrum obtained at 25 °C (cf. cross-peaks for T3 and T10). Again, this is a consequence of the larger line widths at low temperature, which reduces the information present in the spectrum. Quantitative measurements of the couplings at 25 °C and 50 °C are reported in Table 8. The agreement between independent measurements (i.e., from the two cross-peaks involving H1') of the same coupling constant at 50 °C is on the whole good, i.e., typically within 0.5 Hz for both $^3J_{1'2'}$ and $^3J_{1'2''}$. The estimated splittings are similar to those obtained from the DQF-COSY spectra at 50 °C (Table 6), indicating that under these conditions the coupling constants are reasonably well determined. The value of f_S was calculated according to Eq. 5. P_S for these data was then calculated assuming values of $^3J_{1'2'}$ and $^3J_{1'2''}$ of 1.1 Hz and 7.7 Hz, respectively, for $P_N = 9°$ (Van Wijk et al., 1992). The values of $^3J_{1'2'}$ for the S conformation were then calculated by $^3J_{1'2'}(S) = [^3J_{1'2'}(obs) - (1 - f_S)\,^3J_{1'2'}(N)]/f_S$,

TABLE 8
EFFECT OF TEMPERATURE ON SPLITTINGS IN d(CATGTGACGTCACATG)$_2$ MEASURED BY P.E.COSY

Nucleotide	Temperature (°C)	$^3J_{1'2'}$ (Hz)		$^3J_{1'2''}$ (Hz)		$\Sigma_{1'}$ (Hz)	f_S (°)	P_S (°)
		1'2'	1'2"	1'2'	1'2"			
C1	25	8.9	6.1	4.7	7.8	13.8	0.70	117, ns[a]
	50	8.0	nd[b]	5.9	5.8	13.9	0.71	126–162, 126–162
A2	25	10.4	8.3	4.4	8.6	15.9	(1)	90–126, ns
	50	9.5	8.8	5.6	5.7	14.8	0.86	125–162, 120–170
T3	25	11.1	9.0	3.6	9.2	16.5	(1)	100–160, ns
	50	9.2	nd	5.4	5.8	14.8	0.85	126–162, 126–162
T5	25	9.2	9.0	nd	9.6	18.7	(1)	110–170, ns
	50	8.7	8.7	5.7	5.9	14.5	0.8	110/180, 120–170
G6	25	11	nd	nd	nd	nd	nd	ns
	50	10.1	9.8	5.0	5.4	15.2	0.91	126–162, 126–162
C8	25	10	9	5	8.7	16.4	(1)	99/180, ns
	50	8.8	7.8	5.6	6.3	14.3	0.76	115–175, 110–180
T10	25	10	nd	nd	nd	nd	nd	ns
	50	9.5	8.9	5.9	6.1	15.2	0.92	110/175, 110–180
A14	25	9.5	nd	4.3	6.9	15.1	0.9	110–170, 110–170
	50	8.2	8.4	6.2	5.9	14.4	0.78	110–170, 110–170
T15	25	10	8	5.9	8.9	16.4	(1)	95/190, 72/207
	50	8.5	8.4	6.5	6.7	15.1	0.9	100/190, 95/195
G16	25	9.8	8.5	4.8	7.1	15.1	0.9	110/170, ns
	50	7.5	7.4	6.7	6.3	14.0	0.71	108/180, 100/195

Apparent splittings were measured in both halves of the cross-peaks and averaged; f_S was calculated using Eq. 5, and P_S was determined as described in the text. The two entries for P_S correspond to estimates from $^3J_{1'2'}$ and $^3J_{1'2''}$, respectively. Two values are separated by a slash denoting alternative solutions, with errors of ca. ± 18° for each value.

[a] ns = no solution.

[b] nd = not determined.

which was done similarly for $^3J_{1'2''}$. The corrected values were then used to find ranges of P_S consistent with these values. As Table 8 shows, for the data at 25 °C often no solution could be found, or only inconsistent solutions were found. In addition, the precision of the parameters was very low. In contrast, at 50 °C the agreement between the two estimates was generally very good, although there were some ambiguous solutions for which additional information would be needed (see above). The results obtained from analysis of the P.E.COSY data at 50 °C are consistent with the f_S and P_S ranges calculated from other experiments (see above).

Discussion and Conclusions

The results presented above show that data acquired at 50 °C are sufficient to analyse sugar conformations without undue influence of line widths. The main effect of lower temperatures is an increased line width: at 25 °C all of the line widths are approximately twofold larger than at 50 °C. Under these conditions even the narrowest resonances exceed the coupling constants or individual splittings in the spectra, which causes amalgamation or cancellation of nearby lines, depending on whether they have in-phase or antiphase components, and leads to substantial errors in the derived coupling constants. As shown in Table 8, the agreement between independent estimates of coupling constants in P.E.COSY is very poor at 25 °C. This indicates that P.E.COSY does not provide accurate estimates of the coupling constants for long correlation times.

Whilst the analysis of the data at 50 °C is self-consistent and agrees with simulations, the experimental patterns in the COSY cross-peaks at 25 °C do not agree with the simulated patterns. For these simulations, we used line widths expected according to the slower tumbling time. The experimental $T_{1\rho}$ values are in agreement with the expected values, indicating that the dipolar contribution to the line widths has been adequately accounted for. However, reasonable agreement could be obtained only by using much smaller line widths or very different values of the coupling constants. We saw no evidence in the spectra for substantial changes in conformation in the range of 25 °C to 50 °C. Possible alternative explanations include an exchange contribution to some line widths at 50 °C, but not at 25 °C. However, as essentially all of the cross-peaks are affected, this would require that the whole molecule was undergoing a transition in this range, yet the global T_m is > 70 °C. Furthermore, the actual line widths measured at 50 °C agree well with those estimated from the $T_{1\rho}$ experiment, which rules out a substantial contribution from exchange. Zhu et al. (1994) have recently reported that the fine structure of COSY cross-peaks can be distorted at large correlation times, with no significant effect on the sums of the coupling constants. As it is the fine structure that we cannot easily account for, it is possible that the cross correlation between dipolar and scalar effects is responsible at least in part for the observations made at 25 °C, where $\tau_c \approx 6$ ns.

It is clear that under conditions of large overall correlation time the evaluation of proton vicinal coupling constants and sums of coupling constants cannot be obtained by direct measurements from any spectrum. The line width of the peaks appears to play a central role in determining either the peak-to-peak separation or the cross-peak pattern and/or shape of DQF-COSY and P.E.COSY spectra. The limiting effect of the large line width on extracting the coupling constants from NMR data has been reported in several cases, suggesting the spectral simulation approach should be used in order to determine the sugar conformation (Celda et al., 1989; Gochin et al., 1990; Schmitz et al., 1990,1992; Macaya et al., 1992; Majumdar and Hosur, 1992; Schultze et al., 1994). However, some methods for the simulation of multiplet structures of J-coupled spin systems of 2D NMR spectra reported in the literature (Celda et al., 1989; Majumdar and Hosur, 1992) do not systematically consider the influence of line width on the intensity and/or fine structure of cross-peaks. Without independent knowledge, it is difficult to determine simultaneously coupling constants and line widths from the spectra. As we have shown, the line widths for different kinds of protons can be very different and there can be substantial variations for the same kind of proton in different nucleotides (cf. Tables 1 and 2). Assuming a fixed line width for all protons or for each kind of proton is clearly not sufficient. Furthermore, for larger molecules, quite different conformations can produce very similar cross-peak patterns in the COSY experiments if the line widths are allowed to vary within an experimentally based range. The multiplet fine structure is strongly affected by the line width of protons involved either in active or passive coupling, and decreasing the line width can be compensated by increasing ^3J. Under these conditions, line widths and coupling constants cannot be considered as independent parameters. Hence, even iterative fitting of peak shapes where the coupling constants, line widths and frequencies are adjustable parameters (Macaya et al., 1992) may not always produce accurate results for slowly tumbling molecules. It is clear that any simulation method needs a proper adjustment of the line width, and measurement of the actual line widths of H1', H2', H2", H3' and H4' for each sugar ring is necessary to obtain an unambiguous result.

In theory, dipolar transverse relaxation influences the multiplet fine structure (Zhu et al., 1994; Norwood, 1995) when the correlation time becomes large. Under these circumstances, transverse relaxation is not exponential, and much more involved calculations are needed to simulate the multiplet fine structure. Additional relaxation measurements of in-phase and anti-phase components

would also be required for such calculations (Meersmann and Bodenhausen, 1995). For long correlation times (ca. > 6 ns, see above), the line widths are in any case very large, and coupling constants cannot be reliably extracted by simulation, even when ignoring cross-correlation effects.

Simultaneous fitting of coupling constants and intra-sugar proton distances, or using better actual NOE time courses, will improve analysis of the sugar conformation. Where line widths are large such that only $\Sigma_{1'}$ can be measured reliably, intra-ring NOEs and base–sugar proton NOEs are essential to fix the value of P_S to better than the S domain (ca. 90° to 270°). Where the couplings and NOEs indicate that the S conformer is dominant, $\Sigma_{1'}$ provides a good estimate of f_S. In this case, $r_{1'-4'}$ and $r_{2''-4'}$ usually allow tighter limits to be placed on P_S. As pointed out by Wijmenga et al. (1993), this additional information may be less restraining for nucleotides where f_S is about 0.5. In the present case, and in general for B-DNA duplexes (Van Wijk et al., 1992), f_S is higher; typically in the range of 0.8 to 1.0.

In the ATF-2 hexadecamer acceptable sugar conformations could only be analysed using data acquired at 40 °C or higher, where the rotational correlation time is < 3 ns and H1' line widths are < 3 Hz. Larger correlation times (> 5 ns) lead to broad lines, such that the line width of H1' is comparable to the coupling constants, and those of H2' and H2" are much larger than the coupling constants. In our case, at 25 °C the line widths were sufficiently broad that the peak shapes in DQF-COSY all looked remarkably similar, in contrast with the data acquired between 40 °C and 50 °C.

Acknowledgements

This work was supported by the Medical Research Council and the Wellcome Trust Foundation. M.R.C. gratefully acknowledges a Wellcome Trust Fellowship. We thank Drs. Angelo Gargaro and James Feeney for careful reading of the manuscript and helpful discussions.

References

Allerhand, A., Chen, F. and Gutowsky, H.S. (1965) *J. Chem. Phys.*, **42**, 3040–3047.

Bax, A. and Davis, D.G. (1985) *J. Magn. Reson.*, **65**, 355–360.

Bax, A. and Lerner, L. (1988) *J. Magn. Reson.*, **79**, 429–438.

Borer, P.N., LaPlante, S.R., Kumar, A., Zanatta, N., Martin, A., Hakkinen, A. and Levy, G.C. (1994) *Biochemistry*, **33**, 2441–2450.

Celda, B., Widmer, H., Leupin, W., Chazin, W.J., Denny, W.A. and Wüthrich, K. (1989) *Biochemistry*, **28**, 1462–1471.

Conte, M.R., Jenkins, T.C. and Lane, A.N. (1995) *Eur. J. Biochem.*, **229**, 433–444.

Eberstadt, M., Gemmecker, G., Mierke, D.F. and Kessler, H. (1995) *Angew. Chem., Int. Ed. Engl.*, **34**, 1671–1695.

Farmer, B.T., Macura, S. and Brown, L.R. (1988) *J. Magn. Reson.*, **80**, 1–22.

Freeman, R. and Hill, H.D.W. (1971) *J. Chem. Phys.*, **55**, 1985–1986.

Gochin, M., Zon, G. and James, T.L. (1990) *Biochemistry*, **29**, 11161–11171.

Griesinger, C., Otting, G., Wüthrich, K. and Ernst, R.R. (1988) *J. Am. Chem. Soc.*, **110**, 7870–7872.

Jones, C. and Lee, K.A.W. (1991) *Mol. Cell. Biol.*, **11**, 4279–4305.

Koning, T.M.G., Boelens, R., Van der Marel, G.A., Van Boom, J.H. and Kaptein, R. (1991) *Biochemistry*, **30**, 3787–3797.

Lane, A.N., Lefèvre, J.-F. and Jardetzky, O. (1986) *J. Magn. Reson.*, **66**, 201–218.

Lane, A.N. and Forster, M.J. (1989) *Eur. Biophys. J.*, **17**, 221–232.

Lane, A.N. (1990) *Biochim. Biophys. Acta*, **1049**, 189–204.

Lane, A.N. (1991) *Carbohydr. Res.*, **221**, 123–144.

Lane, A.N., Frenkiel, T.A. and Bauer, C.J. (1993) *Eur. Biophys. J.*, **21**, 425–431.

Lane, A.N. and Fulcher, T. (1995) *J. Magn. Reson. Ser. B*, **107**, 34–42.

Lipari, G. and Szabo, A. (1982) *J. Am. Chem. Soc.*, **104**, 4546–4558.

Macaya, R.F., Schultze, P. and Feigon, J. (1992) *J. Am. Chem. Soc.*, **114**, 781–783.

Majumdar, A. and Hosur, R.V. (1992) *Prog. NMR Spectrosc.*, **24**, 109–158.

Meersmann, T. and Bodenhausen, G. (1995) *J. Magn. Reson. Ser. A*, **115**, 277–282.

Mueller, L. (1987) *J. Magn. Reson.*, **72**, 191–196.

Neuhaus, D., Wagner, G., Vasak, M., Kägi, J.H.R. and Wüthrich, K. (1985) *Eur. J. Biochem.*, **151**, 257–273.

Norwood, T.J. (1995) *J. Magn. Reson. Ser. A*, **114**, 92–97.

Piotto, M., Saudek, V. and Sklenář, V. (1992) *J. Biomol. NMR*, **2**, 661–665.

Press, W.H., Flannery, B.P., Teukolsky, S.A. and Vetterling, W.T. (1986) *Numerical Recipes: The Art of Scientific Computing*, Cambridge University Press, Cambridge, U.K., pp. 498–546.

Rinkel, L.J., Van der Marel, G.A., Van Boom, J.H. and Altona, C. (1987) *Eur. J. Biochem.*, **166**, 87–101.

Rinkel, L.J. and Altona, C. (1987) *J. Biomol. Struct. Dyn.*, **4**, 621–649.

Schmitz, U., Zon, G. and James, T.L. (1990) *Biochemistry*, **29**, 2357–2368.

Schmitz, U., Sethson, I., Egan, W.M. and James, T.L. (1992) *J. Mol. Biol.*, **227**, 510–531.

Schultze, P., Smith, F.W. and Feigon, J. (1994) *Structure*, **2**, 221–233.

Searle, M. (1993) *Prog. NMR Spectrosc.*, **25**, 403–480.

Smith, S.A., Levante, T.O., Meier, B.H. and Ernst, R.R. (1994) *J. Magn. Reson. Ser. A*, **106**, 75–105.

States, D.J., Haberkorn, R.A. and Ruben, D.J. (1982) *J. Magn. Reson.*, **48**, 286–292.

Tassios, P.T. and LaThangue, N.B. (1990) *New Biologist*, **2**, 1123–1134.

Tropp, J. (1980) *J. Chem. Phys.*, **72**, 6035–6043.

Van de Ven, F.J.M. and Hilbers, C.W. (1988) *Eur. J. Biochem.*, **178**, 1–38.

Van Duynhoven, J.P.M., Goudriaan, J., Hilbers, C.W. and Wijmenga, S.S. (1992) *J. Am. Chem. Soc.*, **114**, 10055–10056.

Van Wijk, J., Huckriede, B.D., Ippel, J.H. and Altona, C. (1992) *Methods Enzymol.*, **211**, 286–306.

Wijmenga, S.S., Mooren, M.M.W. and Hilbers, C.W. (1993) In *NMR of Macromolecules. A Practical Approach* (Ed., Roberts, G.C.K), IRL Press, Oxford, U.K., pp. 217–288.

Wüthrich, K. (1986) *NMR of Proteins and Nucleic Acids*, Wiley, New York, NY.

Zhu, L., Reid, B.R., Kennedy, M. and Drobny, G.P. (1994) *J. Magn. Reson. Ser. A*, **111**, 195–202.